Toxicology in Vitro 72 (2021) 105095

Contents lists available at ScienceDirect

Toxicology in Vitro

journal homepage: www.elsevier.com/locate/toxinvit

Toxic effects of gunshot fumes from different ammunitions for small arms on lung cells exposed at the air liquid interface

Espen Mariussen [a,b,*], Lise Fjellsbø [a,c], Tomas Roll Frømyr [b], Ida Vaa Johnsen [b], Tove Engen Karsrud [b], Øyvind Albert Voie [b]

[a] Norwegian Institute for Air Research (NILU), PO Box 100, NO-2027 Kjeller, Norway
[b] Norwegian Defence Research Establishment (FFI), PO Box 25, NO-2027 Kjeller, Norway
[c] Norwegian University of Life Sciences (NMBU), PO Box 5003, NO-1432 Ås, Norway

ARTICLE INFO

Keywords:
Gunshot fumes
Nanoparticles
Air liquid interface
Comet assay
Lung deposition factors

ABSTRACT

Concerns have been raised as to whether gunshot fumes induce prolonged reduced lung capacity or even cancer due to inhalation. Gunshot fumes from three different types of ammunition calibre 5.56 mm × 45 NATO were investigated. SS109 has a soft lead (Pb) core, while NM255 and NM229 have a harder steel core. Emissions from ammunitions were characterized with respect to particle number- and mass-size, and mass distribution, heavy metal content, and different gases. Lung epithelial cells were exposed to the fumes at the air liquid interface to elucidate cytotoxicity and genotoxicity. Irrespectively of ammunition type, the largest mass fraction of generated particulate matter (PM) had a size between 1 and 3 μm. The highest number of particles generated was in the size range of 30 nm. Fumes from NM255 and NM229 induced cytotoxic effects of which the emission from NM229 induced the highest effect. Fumes from NM229 induced a dose-related increase in DNA-damage. Significant effects were only achieved at the highest exposure level, which led to approximately 40% reduced cell viability after 24 h. The effect probably relates to the mass of emitted particles where the size may be of importance, in addition to emission of Cu and Zn. A complex mixture of chemical substances and PM may increase the toxicity of the fumes and should encourage measures to reduce exposure.

1. Introduction

Gunshot fumes from firing small arms contain a complex mixture of gases and aerosols, consisting of both particulate matter (PM) and liquids. The fumes are produced from the ignition of the primer and the propellants, and from the friction between the bullet and the barrel of the gun. In 2003, the Norwegian armed forces changed their primary assault rifle to the HK416 (Heckler & Koch, Germany). Shortly after the new weapon was put into service, flu like symptoms after training sessions at firing ranges were reported. It became evident that the symptoms were due to exposure to gunshot fumes. The symptoms were similar to what previously have been observed among welders (Voie et al., 2014). The symptoms were attributed to the newly introduced ammunition with a steel core instead of a lead (Pb) core, and further use of this ammunition type was temporarily prohibited.

The rational for replacing the traditional lead core bullets with the steel core bullets by the Norwegian armed forces in 2003, was to reduce both the environmental load of Pb contamination and the shooters exposure to Pb. Several studies have shown that exposure to Pb during training increases the level of Pb in the blood. In addition to exposure from training at firing ranges, there are also raised concerns about long-term effects of Pb exposure from consumption of game (Goldberg et al., 1991; Valway et al., 1989; Fischbein et al., 1979; Fachehoun et al., 2015; Laidlaw et al., 2017). Investigations revealed that the newly introduced steel core ammunition, NM229, generated firearm discharge fumes with more copper (Cu) and zinc (Zn) than the lead core ammunition, SS109, that it replaced (Strømseng et al., 2009; Dullum et al., 2015). This is mainly caused by a higher friction between the barrel and the bullet due to the higher radial stiffness of the steel core and, consequently, a lesser ability to deform while passing through the barrel (Dullum et al., 2015). Both types of bullets are jacketed with an alloy of Cu (90%) and Zn (10%). The increased emission of Cu and Zn was particularly prominent when used in the HK416 compared to other small arms of different calibres, such as the AG3. The barrel of HK416 is narrower than the barrel of AG3, which increases the friction between the bullet and the barrel, leading to higher concentrations of gunshot aerosols (Dullum

* Corresponding author at: Norwegian Institute for Air Research (NILU), PO Box 100, NO-2027 Kjeller, Norway.
E-mail address: espen.mariussen@nilu.no (E. Mariussen).

https://doi.org/10.1016/j.tiv.2021.105095
Received 30 July 2020; Received in revised form 18 December 2020; Accepted 11 January 2021
Available online 14 January 2021

et al., 2015). NM255 was designed with the goal of decreasing the contact area between the bullet and the barrel compared to NM229. According to the manufacturer this ammunition has less emission of suspended dust particles and exhaust gases (Nammo, 2012; 2014).

In a study by Voie et al. (2014), volunteers were exposed to gunshot fumes from the two ammunition types with steel core, NM229 and NM255, in addition to the leaded SS109 in order to compare health effects induced by gunshot firing. The main findings showed that all three ammunition types induced temporarily, but prominent health effects such as fever, coughing, increased C-reactive protein (CRP) in blood and reduced lung function, similar to the symptoms from metal fever (Voie et al., 2014; Borander et al., 2017; Sikkeland et al., 2018). In addition, carbon monoxide (CO) in the fumes led to increased levels of carboxyhemoglobin in the blood of the exposed shooters (Voie et al., 2014). CO-poisoning may lead to headaches and seriously decrease judgment and performance.

The gunshot fumes consist of complicated mixtures of PM, gases, and aerosols of different chemical origin. The PM contains metals orginating from the bullet and the primer, such as Zn, Cu, Pb and iron (Fe). There will be formed combustion products from the gunpowder, such as soot and trace amounts of poly aromatic hydrocarbons (PAHs), in addition to gases such as CO, CO_2, H_2O, CO, HCN, NH_3, NO_x, SO_2 and HCl (Wingfors et al., 2014; Aurell et al., 2019). It has been shown that more than 90% of the total amount of particles produced have diameters less than 30 nm (Wingfors et al., 2014; Aurell et al., 2019). A major concern is if repeated exposure to gunshot fumes may lead to harmful effects in the long term. These effects may include chronic pulmonary effects and even cancer, which may be induced by DNA-toxic substances such as PAHs. A study by Palmer et al. (1994) showed that emissions from the M16 rifle were mutagenic in the Salmonella/Ames test. The effect was associated with the nanosized particles.

To elucidate the genotoxic potential of gunshot fumes, we exposed lung cells at the air liquid interface (ALI) to the fumes derived from the three aforementioned ammunitions, NM255, NM229 and SS109. Genotoxicity was elucidated by the comet assay, which is a widely used method to detect DNA breaks *in vitro* as well as *in vivo* (Collins et al., 2008). A modified version of the comet assay using the lesion-specific enzyme formamidopyrimidine DNA glycosylase (Fpg) was used to detect oxidized purines, which is an indicator of oxidative stress induced DNA lesions (Collins et al., 1996). The cytotoxic effect of the smoke was tested to compare the general toxicity of the different ammunition types. The generated gunshot fumes were subjected to physical and chemical characterization with respect to particle mass- and number-size distribution. Collected PM were analysed for Cu, Zn and Pb. In addition, the gasses CO_2, CO, NH_3, HCN and NOx. were measured by Fourier transform infrared spectroscopy (FTIR).

2. Materials and methods

2.1. Collection of gunshot fumes

A standard HK416 (Heckler & Koch, Germany) assault rifle was carefully attached in a frame adjacent to a second frame (Dullum et al., 2015, Fig. 1S, Supplementary). An antistatic polyethylene sheet (P/P 50mu Elfa Distrelec) was wrapped around the frames and the rifle creating a chamber with a volume of approximately 1 m^3. The frame where the rifle was attached contained a hole sealed with a glove, which enabled firing of the rifle without leakage of the emitted fumes. Shots were fired through a port covered with a rubber sheet in the opposite frame. The rubber sheet efficiently kept the leakage of emitted fumes from the exit hole to a minimum. A number of one to ten shots were fired. If more than one shot was fired, the shots were fired in a quick succession. Three ammunition types of calibre 5.56 mm × 45 NATO were tested, NM229, NM255 and SS109, all manufactured by NAMMO (Norway). The main difference between the NM255 and NM229 ammunitions is a different geometry of the NM255 bullet, resulting in a smaller contact area between the bullet and the gun barrel compared to NM229.

2.2. Measurements of gases and sampling of emitted particles

Within the chamber in which the fumes were collected, an Aerosol Analysis Monitor (37 mm, Millipore) was attached and connected to an air sampler (SKC AirChek XR5000 sample pump), which collected air at a rate of 2 L/min. The monitor is a transparent disposable plastic filter holder assembled with a filter for air sampling. PM was sampled for 15 min on a 0.4 μm isopore membrane filter (Millipore), which was weighed and subjected to further chemical analysis. Emission factors were calculated for each analysed element and PM according to Wingfors et al. (2014). The emission factor E (unit mass/round) was calculated as the measured mass collected on the filter divided by the volume of sampled air (C/30 L) multiplied by the volume of the test chamber V (1000*L*), divided with numbers of rounds (n). Different gasses (CO, NH_3, HCN and NOx, CO_2, CH_4, H_2O, SO_2) emitted from the shooting were measured by a Gasmet DX4015 portable Fourier transformed infrared spectroscopy (FTIR).

In separate experiments, the physical characterization of the emitted aerosols was conducted by a Fast Mobility Particle Sizer spectrometer (FMPS) (TSI, Model 3090) and a low pressure impactor (DLP) (Dekati®, DLPI+). The FMPS does real-time measurements of particles in a size range between approximately 6 nm and 500 nm in a total of 32 channels with a resolution of one second. The DLPI impactor has 13 stages, which collect airborne particles in a size range between approximately 30 nm and 10 μm. The impactor was operated with a flow rate of 10 L/min and particles were collected on pre-weighed and greased (Dekati DS-515 Collection Substrate spray) polycarbonate filter traps (Whatman, Nucleopore® Polycarbonate) placed on each stage of the impactor. The impactor and the FMPS were initiated prior to the firing of three consecutive rounds with approximately 60 s between each round. Before entering the FMPS the fumes were diluted by a factor of 10 with a TSI aerosol diluter. The collection of particles on the impactor was terminated 5 min after the last round was fired. Each filter trap from the impactor was weighed and then subjected to chemical analysis as described below.

2.3. Analysis of elements on filters

Filters from the impactor and the Aerosol Analysis Monitor were transferred to Teflon containers and digested in an UltraWave® SRC (Milestone) pressurized microwave oven with 5 mL 65% ultra-pure nitric acid and 5 mL ultra-pure MilliQ-water for 15 min at 220 °C. The samples were then diluted to 50 mL by ultra-pure MilliQ water and subjected to element analysis. The extracts were analysed for the elements Cu, Zn, Pb, Sb, Fe, manganese (Mn), Aluminium (Al) and barium (Ba) with an inductively coupled plasma spectrometer (ICP-MS, Thermo X-series II). An internal standard and a four-point standard curve were used for the quantification of elements in the samples (0.1–1000 μg/L). Representative detection limits for the elements in water, estimated as mean + 10 times the standard deviation of the blanks from 7 analytical runs (Armbruster et al., 1994), were 0.13 ± 0.09 μg/L, 0.20 ± 0.11 μg/L, 0.11 ± 0.13 μg/L, 0.11 ± 0.15, 1.4 ± 1.0 μg/L, 0.03 ± 0.01 μg/L, 2.0 ± 0.90 μg/L for Cu, Zn, Sb and Pb, Al, Mn and Fe, respectively. To ensure correct quantification a reference solutions of known metal concentration (TM 23.3 and TMDA 61.2, Environment Canada, Canada) were analysed. A deviation of 5% from the given concentration in the reference solution was accepted. Blanks were regularly analysed to control background contamination.

2.4. Cell cultivation

The human epithelial cell line, A549 (ATCC), was cultivated in Dulbecco's Modified Eagle's Medium (DMEM) including 10% foetal

bovine serum (FBS), penicillin (100 U/mL) and streptomycin (100 μg/mL) and kept in a CO_2 incubator at 37 °C. The cells were routinely subcultured by trypsinization every second day or when they reached a confluency of about 70–80%. For the ALI experiments, 200,000 cells were transferred to 6-well cell culture inserts (Falcon, 0.45 μm membranes), which has a cell growth area of 4.2 cm^2. After 2 days, the cells reached confluency and were prepared for exposure. The cell culture inserts were put into the wells of a preheated Vitrocell module (37 °C) with culture medium. Immediately before exposure, the culture medium was removed from the cells and put into ALI conditions. The exposure module was assembled according to the manufacturer, and the cells were exposed to emitted gunshot fumes or ambient air for 15 min. After exposure, 1 mL of pre-warmed culture medium was added to the cells. The exposed cells were then either immediately subjected to comet analysis or put in an incubator for 24 h for a subsequent cell viability experiment.

2.5. Exposure of gunshot fumes on cells at ALI

Within the chamber, in which the gunshot fumes were collected, a rubber tube (5 mm inner diameter) was attached leading the smoke at a rate of 4 L/min by a vacuum pump to a Vitrocell® 6/4 *CF* base module for direct exposure of cell cultures to airborne substances (Fig. 2S). The vacuum pump was started immediately before the shots were fired. Within the module, the fumes were split and led to the wells at a rate of 5 mL/min. Adjacent to the wells with the cells, the 6/4 *CF* base module had a balance to estimate the mass of deposited particles. In addition, ambient air was filtered through a 0.45 μm HEPA filter and transferred by vacuum at a rate of 5 mL/min to a Vitrocell® 6/3 *CF* base module. The cells exposed to ambient air were used as negative controls. At least four separate experiments were performed for each assay with three different ammunitions in addition to the negative controls that were exposed to ambient air. Doses were defined as number of shots. The exposure modules contain three wells with cell inserts, which implies that three repeats were made from each separate experiment. Since cells grown in ALI condition may be subjected to increased stress, additional controls were included with cells cultivated on inserts under submerged conditions.

2.6. Cell viability assessment with MTT

Cell viability was assessed with the MTT-assay (Dalen et al., 2009). The exposed cells were washed once with pre-warmed phosphate-buffered saline (PBS) and added 1 mL of MTT (0.5 mg/mL 3-[3,5-dimethylthiazol-2-ul]-2,5-diphenyltetrazolium bromide, Sigma Aldrich, St. Louis, MO) dissolved in PBS added glucose (5.5 mM). After approximately one hour of exposure, the MTT solution was removed, and 1 mL of dimethyl sulfoxide (DMSO) was added to each cell culture insert to dissolve the reduced MTT. An aliquot of the DMSO solution was then transferred to a transparent 96-well plate for reading of absorbance in a Tecan (Sunrise) microplate reader at 570 nm with background at 690 nm subtracted.

2.7. Comet assay with concomitant trypan blue assay and relative cell growth assay

Approximately 5 to 10 min after the 15 min exposure to the emissions, the cells on the inserts were detached by trypsinization and dissolved in DMEM. A small aliquot of the cell suspension (10 μL) was mixed with trypan blue (10 μL), and the cell number and the cell viability were estimated in a Countess cell counter. Relative cell growth was estimated by seeding viable cells (20,000 cells/well) on 6 well plates followed by incubation for 48 h. After 48 h the cells were trypzinized and counted on a Countess cell counter. Relative cell growth was calculated by dividing total cell growth of exposed cells with unexposed cells.

The comet assay was performed on 12-gel microscope slides for increased throughput as described by El Yamani et al. (2017). One volume of cells was mixed with four volumes of low melting point agarose (0.8% in phosphate buffered saline, (PBS)) at 37 °C. From this mixture 10 μL (approximately 400 cells) were put on cold glass microscope slides pre-coated with 0.5% standard melting point agarose. Four mini gels were prepared from each cell culture insert on two separate microscope slides, one slide for regular comet and one slide that was treated with the lesion-specific enzyme formamidopyrimidine DNA glycosylase (Fpg). Three cell culture inserts were treated simultaneously, which means that12 mini gels from three repeats were added to each glass microscope slide. After a few minutes at 4 °C in the fridge to allow the gels to set, the microscope slides were put into a cold lysis solution (2.5 M NaCl, 0.1 M EDTA, 10 mM Tris, 10% Triton X-100, pH 10) in the fridge overnight. After lysis, the slides were placed in an alkaline solution (0.3 M NaOH, 1 mM EDTA) for 20 min, followed by electrophoresis at 1.25 V/cm for 20 min in a horizontal electrophoresis tank. The slides were then washed in PBS followed by water and allowed to dry. The slides were stained with SybrGold® (Invitrogen) diluted at 1 μL/mL in tris buffer (10 mM Tris–HCl, 1 mM Na2 EDTA, pH 7.5–8), covered with a cover slip and examined under a fluorescence microscope (Leica DMI 6000 B). Images of comets were scored using the Comet Assay IV software (Perceptive Instruments). The median % tail DNA from 50 comets was estimated as the measure of DNA damage.

For DNA base oxidation detection, a modified comet assay was applied by inclusion of a post-lysis incubation with Fpg that recognizes oxidized purines, and converts them to strand breaks (Collins et al., 1996). After lysis, the slides were washed with a Fpg buffer (40 mM HEPES, 0.1 M KCl, 0.5 mM EDTA, 0.2 mg/mL BSA, pH 8.0). Approximately 30 μL of Fpg (a gift from Professor Andrew Collins, University of Oslo, Norway) diluted in the Fpg-buffer was added onto each gel. The slides were covered with polypropylene film and incubated for 30 min at 37 °C in a humidified box. After the enzyme treatment, the slides were incubated in alkaline solution and electrophoresed as described above.

Four separate comet experiments were performed studying the effect from the three different ammunition types at three dose levels. For each experiment, positive (H_2O_2) and negative controls (submerged in medium and exposed to ambient air) were included. The exposure module contains three wells with cell inserts, which means that three repeats were made from each separate experiment.

2.8. Statistics

Statistical differences between treatment groups in the cell viability assay and the comet assay were calculated by one-way ANOVA followed by Dunnet post-test. Statistical differences between emission from the different types of ammunition were calculated by two-way ANOVA followed by Tukey's multiple comparison test. The statistics were computed in GraphPad Prism 7. Mathematical calculations, such as mean and standard deviations from the chemical analyses, and size and distributions of particles were calculated in Excel 2013. Deposition factors of CuO, ZnO, Pb and soot (black carbon) in different regions of the pulmonary system were calculated according to the Multi-Path Particle Dosimetry model (MPPD v3.4, Ara, US) (Anjilvel and Asgharian, 1995).

3. Results

3.1. Emission of gases from gunshot fumes

The emission of the gases (CO, CO_2, NH_3, CH_4, NO) increased proportionally with the number of shots (Fig. 1, Fig. 3S). Except for CO, NM255 emitted significantly less of the measured gases compared to the other two ammunition types.

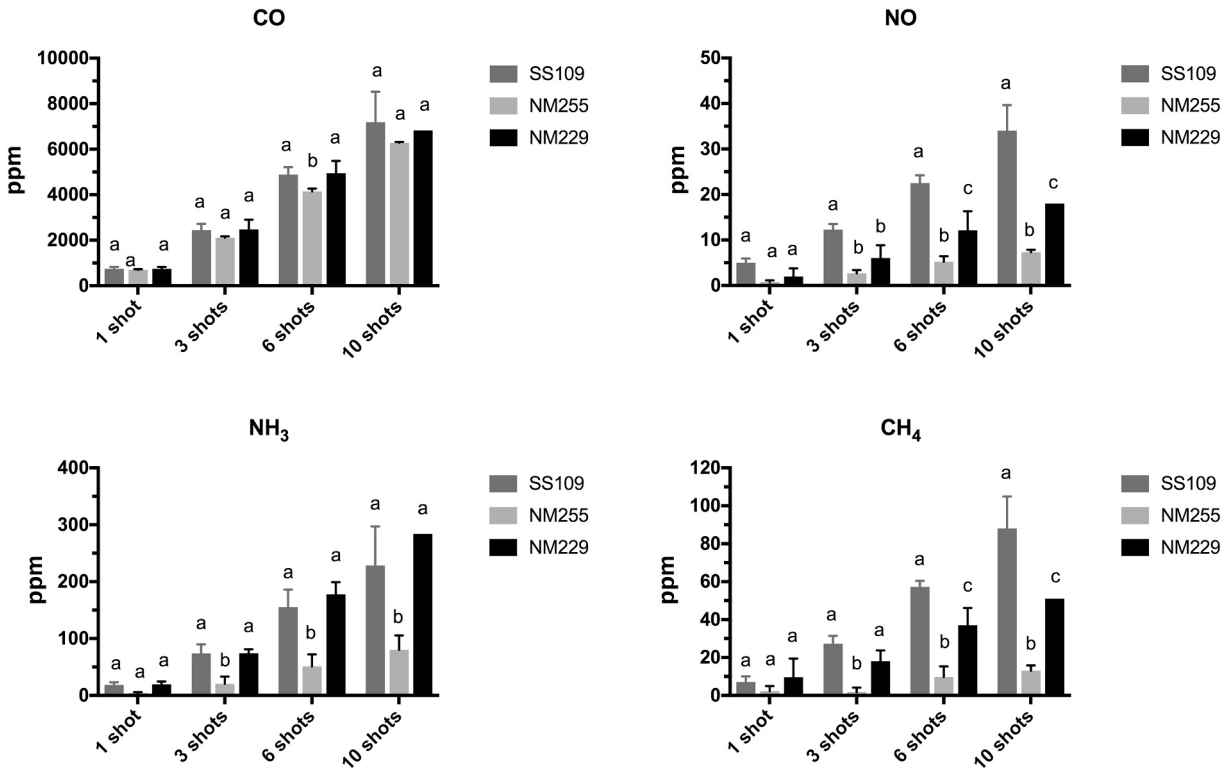

Fig. 1. Emission of CO, NO, NH_3 and CH_4 from three different types of ammunition fired by the HK416 rifle inside the test chamber approximately 7 min after firing the shots. The measured concentrations of the gases are the mean (± SD) of 3 (NM255) or 4 separate measurements (SS109 and NM229). Emission from the three ammunition types where compared statistically with respect to number of shots. Different letters labelled on the bars within each group of shots indicate statistical different emissions of the respective gases between the different types of ammunition analysed by two-way ANOVA followed by Tukey's multiple comparison test ($p \leq 0.05$).

3.2. Emission of metals and particles

Analyses of the filters from the air sampler collecting PM within the shooting chamber showed that, NM229, emitted considerably more Cu and Zn than the two other ammunition types, shown as mass per round and mass per m^3 (Fig. 2, Table 1). NM229 also emitted a slightly larger amount of PM than the other two ammunition types. As expected, SS109 emitted considerably more Pb than the ammunitions with unleaded bullet cores (NM255 and NM229).

3.3. Particle characterization of the gunshot fumes

The impactor collected PM in a size range between approximately 30 nm and 10 μm. The largest portion of PM in the fumes was in the size range between 1 and 3 μm (Fig. 3). In addition, the NM229 mass-size distribution had a mode between 200 and 300 nm. A similar bimodal pattern was observed for both NM255 and SS109, but less distinct. Each stage from the impactor was analysed for Cu, Zn and Pb. The content of Zn in the fumes showed approximately the same bimodal pattern as the particle mass distribution (Fig. 4). In comparison, the Cu mass-size distributions showed only a single large mass fraction peak at 1 μm for all of the ammunition types. The measured emissions of Zn and Cu were much higher for NM229 than the other ammunitions, which are in line with filter sample measurements (Fig. 2, Table 1) The emission of Pb from SS109 appeared to have a unimodal distribution, somewhat broader than the corresponding distribution for Cu (Fig. 4). Pb mass-size distributions for NM229 and NM255 did not show a clear log-normal distribution in the measured size interval. However, the Pb concentrations are low, and the uncertainties in the measurements are significant to the overall shape of the distribution.

The FMPS measures the number-size distribution of emitted particles at one hertz. The measurements with the FMPS showed a unimodal size range between 30 and 80 nm. Immediately after firing the shot, the highest number of particles peaked at approximately 40 nm independent of the ammunition type. After 30 s, and subsequently 60 s, the number of particles decreased considerably, while the size distribution shifted towards larger particles. The mode at 60 s was at approximately 50 nm, 60 nm and 70 nm from NM255, SS109 and NM229 respectively (Fig. 5). Unsurprisingly, the measurements indicates that there is a rapid agglomeration of particles, with only slight differences in kinetics within the observed time, for the three ammunitions.

3.4. Particle deposition on the cell inserts in the lung exposure module

A microbalance was placed within the exposure module, which monitored deposited particles during the experiment. The amount deposited on the microbalance is in principle equivalent to the deposition on the cells. Deposition of fume residues on the balance increased proportionally with the number of shots. Table 2 shows the mass of PM from the gunshots deposited on the microbalance within the Vitrocell exposure module and the equivalent theoretical particulate air concentration. The theoretical particulate air concentrations are crude approximations and are calculated from the mass deposited on the balance after 15 min of exposure with a flow rate of 5 mL/min.

3.5. Cell viability assessment with MTT

Emissions from NM229 and NM255 induced significantly reduced cell viability after exposure to gunshot fumes from 6 and 10 shots (Fig. 6). The effect on the cell viability was, in addition, estimated as a function of deposition of particles measured on the microbalance. The fumes from NM255 appeared to be more toxic to the cells compared to

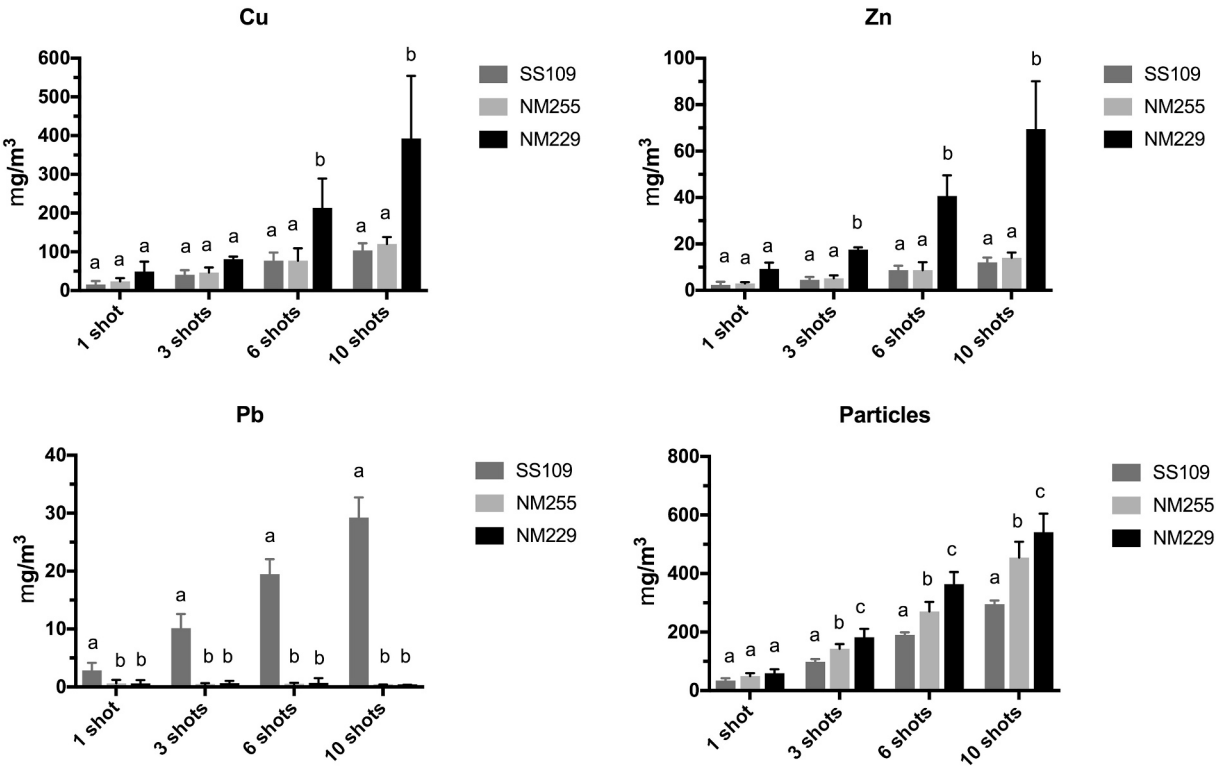

Fig. 2. Estimated concentrations of Cu, Zn, Pb and PM in the gunshot fumes sampled on filters from the aerosol Analysis Monitor with a vacuum pump at a rate of 2 L/min for 15 min (mean ± SD). The measured metal concentrations are the mean of 3 to 6 separate measurements (± SD). The ten shots of NM255 is the mean of two separate measurements, whereas the three shots of NM229 is the mean of seven separate measurements. The measured levels of PM are the mean of 5–8 separate measurements except for the ten shots of NM255 and SS109, which represents the mean of 4 and three measurements respectively. Emissions from the three ammunition types where compared with respect to number of shots. Different letters labelled on the bars within each group of shots indicate statistical different emissions between the different types of ammunition analysed by two-way ANOVA followed by Tukey's multiple comparison test ($p \leq 0.05$).

Table 1
Calculated emission factors for the PM (PM) and metals released by the firing of different ammunition types with a standard HK416 assault rifle in the test chamber.Numbers in brackets are no of measurements.

	NM229	NM255	SS109
PM (mg/round)	59.2 ± 9.6 (26)	47.3 ± 6.8 (25)	32.5 ± 4.9 (22)
Cu (mg/round)	38.1 ± 16.6 (16)	16.8 ± 7.0 (14)	13.7 ± 5.6 (21)
Zn (mg/round)	7.2 ± 2.1 (16)	2.0 ± 0.79 (14)	1.7 ± 0.85 (21)
Pb (mg/round)	0.17 ± 0.37 (16)	0.25 ± 0.39 (14)	3.1 ± 0.86 (21)
Sb (μg/round)	61 ± 96 (16)	69 ± 116 (14)	263 ± 191 (21)
Fe (μg/round)	153 ± 43 (15)	53 ± 19 (14)	124 ± 28 (21)
Mn (μg/round)	1.4 ± 1.3 (16)	0.94 ± 0.52 (14)	2.7 ± 1.3 (21)
Al (μg/round)	78 ± 22 (16)	141 ± 67 (14)	105 ± 99 (21)
Ba (μg/round)	89 ± 89 (16)	96 ± 117 (14)	577 ± 187 (21)

the fumes from NM229. The fumes from NM229 deposited much more particles on the cells but had relatively less effect on the cell viability (Fig. 4S).

3.6. Comet assay with concomitant trypan blue assay and relative cell growth assay

Cells at the ALI exposed to ambient air for 15 min showed a small but significant increase in strand brakes compared to submerged cell cultures (Fig. 7A). Only cells exposed to emission from NM229 showed a significant dose related increase in DNA strand breaks. A similar trend was observed on cells exposed to emissions from NM255, but the effect was not statistically significant (Fig. 7C). Cells exposed to emissions from SS109 were not significantly affected (Fig. 7D). The cells treated with Fpg, which primarily detects oxidized purines, showed no significant additional net increase in strand breaks (Fig. 5S, supplementary)

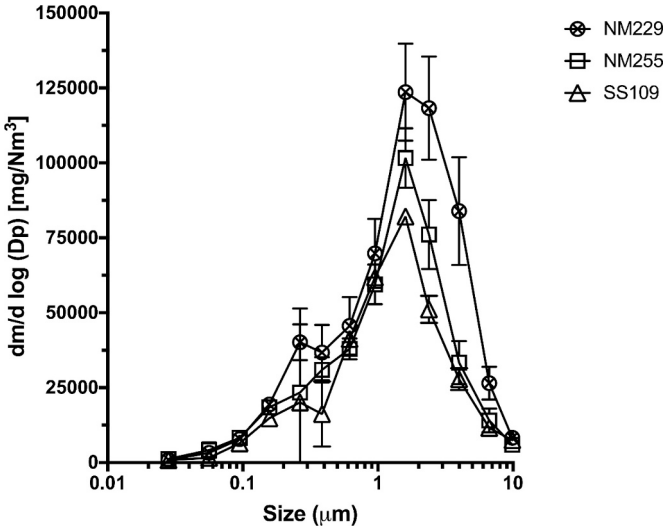

Fig. 3. The mass size distribution of the emitted fumes from the three ammunition types. The impactor was initiated just prior to the firing of three consecutive rounds with approximately 60 s between each round. The collection of particles on the impactor was stopped 5 min after the last round was fired. The results are shown as mean (± SD) of 3 (SS109) or 6 separate experiments (NM255 and NM229).

due to removal of 8-hydroxyguanine (8-OHgua). There was, however, an increasing, but not significant, trend of oxidized bases as a function of concentration in the cells exposed to fumes from SS109 (Fig. 5S, Spearman correlation, $p = 0.083$). The trypan blue exclusion assay did

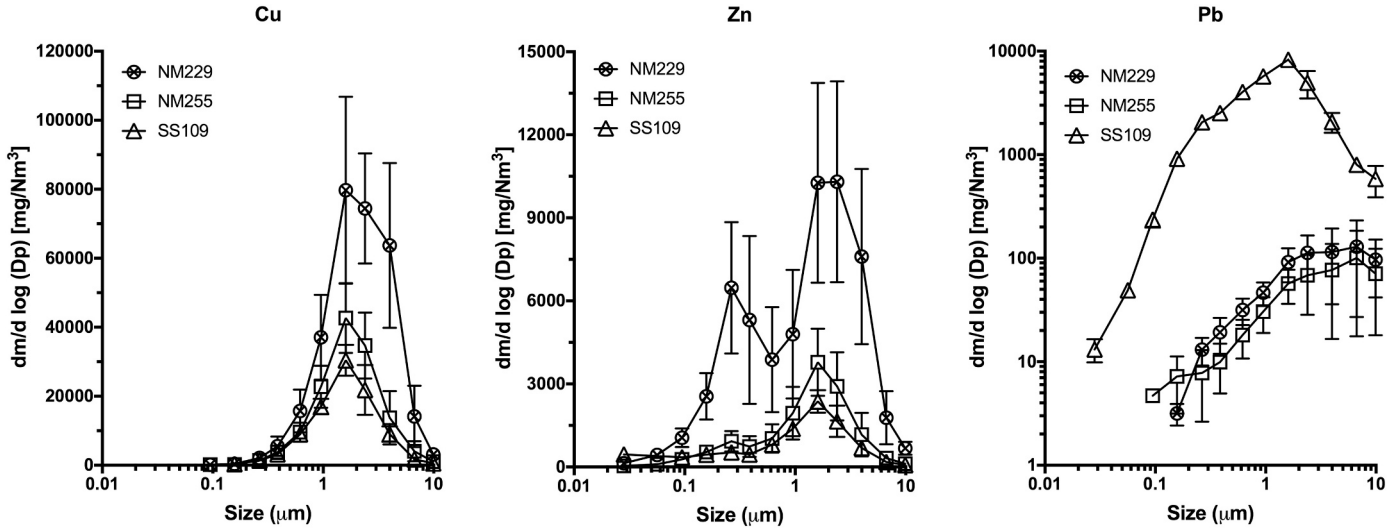

Fig. 4. The mass distribution of Cu, Zn and Pb in the fumes from the three different ammunition types collected on the impactor with respect to particle size. The impactor was initiated just prior to the firing of three consecutive rounds with approximately 60 s between each round. The collection of particles on the impactor was stopped 5 min after the last round was fired. The results are shown as mean (± SD) of 3 (SS109) or 6 separate experiments (NM255 and NM229).

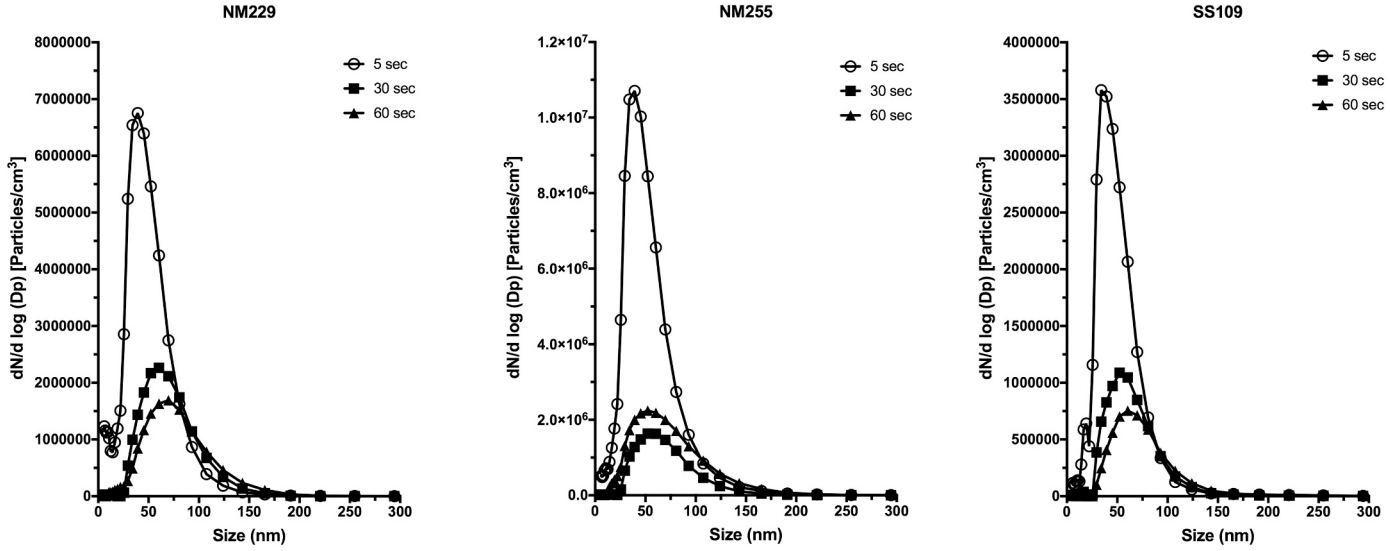

Fig. 5. Size and number distribution of particles in the fumes emitted from one shot of the different ammunition types after 5, 30 and 60 s respectively. The particles were measured in the chamber by FMPS and each data point represents the mean of three (SS109) or 6 separate experiments (NM255 and NM229).

Table 2
The mass of PM deposited on the microbalance within the exposure module (mean ± SD) and the equivalent PM air concentration (mean ± SD). Gunshot fumes were delivered into the module at a rate of 5 mL/min in 15 min. The mass deposited on the microbalance is regarded equivalent to the mass deposited on the cell inserts. Numbers in brackets are no of measurements.

	NM229		NM255		SS109	
	μg/cm^2	mg/m^3	μg/cm^2	mg/m^3	μg/cm^2	mg/m^3
1 shot	0.30 ± 0.10 (8)	17 ± 6.2 (8)	0.18 ± 0.04 (8)	10 ± 2.2 (8)	0.11 ± 0.02 (9)	6.0 ± 1.2 (9)
2 shots	0.83 ± 0.30 (5)	47 ± 17 (5)	0.27 ± 0.05 (4)	15 ± 2.7 (4)	0.20 ± 0.03 (5)	11 ± 1.5 (5)
3 shots	0.76 ± 0.06 (7)	43 ± 3.4 (7)	0.38 ± 0.15 (8)	21 ± 8.3 (8)	0.23 ± 0.06 (8)	13 ± 3.4 (8)
6 shots	1.6 ± 0.44 (8)	93 ± 25 (8)	0.65 ± 0.27 (8)	36 ± 15 (8)	0.33 ± 0.15 (8)	19 ± 8.1 (8)
10 shots	2.0 ± 0.29 (5)	112 ± 16 (5)	0.97 ± 0.51 (4)	55 ± 29 (4)	0.48 ± 0.17 (5)	27 ± 9.7 (5)

not show any significant effect on the cell viability immediately after the exposure (Fig. 7). The relative cell growth assay did not show any significant effect of the exposure, but the cells exposed to the NM229 fumes showed a concentration dependent decreasing trend in viability (Fig. 6S).

4. Discussion

The small arms ammunitions used in this investigation consisted of a cartridge with a propellant and a projectile with a metal core of steel or lead, jacketed with a copper (90%) and zinc (10%) alloy, and a primer,

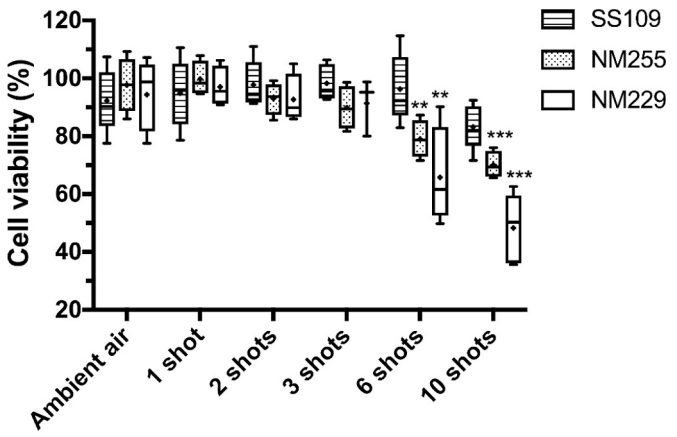

Fig. 6. The effect on cell viability on A549 cell after exposure to shot gun fumes from different types of ammunition. Different numbers of shots were fired into the test chamber and the fumes were transferred onto the cells in the exposure module by vacuum at a rate of 5 mL/min. Results are presented as box plot, with range, median, mean (+) and percentiles from 4 independent experiments performed in triplicates. Asterisks indicate significant different effects on cell viability compared to ambient air analysed by one-way ANOVA followed by Dunnet post test (**$p < 0.01$, ***$p < 0.001$).

which ignites the propellant. The gases, such as CO, CO_2, NO, NH_3 and CH_4, measured in these experiments are primarily combustion and decomposition products from the propellants and the primer. Nitrous gases, such as NO, may also be formed by reaction with atmospheric nitrogen and oxygen immediately after firing. The high concentration of CO compared to the emission of CO_2 (Fig. 3S) indicates a deficiency in oxygen during the gunpowder combustion, which is reasonable bearing in mind the fast combustion process and high temperature following the firing of the weapon (Wingfors et al., 2014). We observed a CO:CO_2 ratio (mole/mol) between approximately 1 and 2 (Fig. 7S), whereas Wingfors et al. (2014) observed an even higher ratio of 5. The mean emission of NO, CH_4 and NH_3 from the unleaded NM255 were 5, 5.9 and 3.6 times lower than the SS109 respectively, and 2.5, 3.9 and 4.4 times lower than for NM229 respectively (Fig. 1), which probably attributes to a different composition of the propellants.

The air samples from the test chamber revealed that the concentration of Cu in the fumes was approximately one order of magnitude higher than for Zn, which reflects the composition of the alloy in the jacket. (Fig. 2, Table 1). Metal analysis of the PM sampled from the firing of shots showed considerable differences between the ammunition types. The unleaded NM229 emitted 2.5 (NM255) and 2.9 (SS109) times as much Cu and 4 (NM255) and 4.5 (SS109) time as much Zn than the other two ammunition types (Fig. 2). The elevated emissions of Cu and Zn from the NM229 ammunition is attributed to a higher friction between the bullet and the barrel of the gun (Dullum et al., 2015). The NM229 also released higher amounts of PM in total with factors of 1.3 and 1.8 times higher emission than NM255 and SS109, respectively (Fig. 2). Much of the particles collected on the filters were probably soot from the propellant. Both steel and leaded ammunition were used with the same rifle, which probably can explain the reason why there was observed Pb in the fumes also from the steel ammunitions. The measured emission factors of Cu and Zn, in addition to other metals and PM, are in accordance with the emission factors measured by Wingfors et al. (2014). They measured emission from standard unleaded ammunition (Sk ptr 5B, 5.56 mm) while using an Ak5 Swedish Armed Forces service rifle. Apart from Pb, they observed similar emissions to the SS109 ammunition tested in this study.

A low-pressure impactor characterizes the mass-size distribution of PM in aerosols. As shown in Fig. 3, the largest mass fraction of PM in the fumes from the three ammunition types was between 1 and 3 μm. There was also a large mass fraction between 200 and 300 nm in the gunshot fumes from the NM229 ammunition. The particle size distributions for NM255 and SS109 also exhibited a shoulder towards smaller particles, although less distinct, indicating a bimodal distribution. Each size fraction from the impactor was analysed for Cu, Zn and Pb. The content of Zn from the NM229 ammunition showed approximately the same bimodal pattern as the particle size distribution with two modes around 250 nm and 1 μm (Fig. 4). A similar, but less distinct bimodal mass size distribution was also observer for Zn from NM255 and SS109. The bimodal mass-size pattern from the ammunitions may be due to the combination of emission of Zn from the primer in addition to the abrasion of the jacket (Dullum et al., 2015). The composition of the NM255 primer is not given, but the NM229 bullet has Sintox as its primer, which is composed of zinc peroxide, tetracene and diazole (Dullum et al., 2015; Brede et al., 1996). The SS109 bullet has Sinoxid as primer, which contains lead styphnate, barium nitrate and antimony sulphide. The SS109 bullet had a higher emission of Ba compared to the other ammunition types showing that the gunshot fumes contain PM with an origin from the primer (Table 1). The mass-size distribution of Cu did not show a similar bimodal pattern. The mass-size pattern of Cu may be attributed to the friction between the barrel and the bullet only.

Measurements with the FMPS showed that the highest number of PM and aerosols generated immediately after the firing of a gunshot was in the size range of approximately 30 nm. After 30 s the highest number of particles was in the size range of approximately 60 nm, indicating a fast and extensive agglomeration of the generated particles. After 60 s the highest number of particles was in a similar size range as after 30 s, indicating that agglomeration of the particles appears to slow down or stabilize. These observations are in line with previous findings (Wingfors et al., 2014; Grabinski et al., 2017; Aurell et al., 2019). Aurell et al. (2019), observed a bimodal mass distribution with a dominance of particles smaller than 30 nm followed by a rapid aggregation to micro-sized particles. Wingfors et al. (2014) showed that more than 90% of the PM produced immediately after firing a round have aerodynamic diameters less than 30 nm. After 12 min it was shown that approximately 75% of the particles still had aerodynamic diameters less than 0.61 μm. Due to agglomeration of the particles the mass fraction of the coarser particles increased, and after 12 min they showed a predominant mass fraction at 1.5 μm and a secondary mass fraction peak at approximately 300 nm. This is similar to our observation with the impactor measurements.

The gunshot fumes were led through a tube with a vacuum pump into the exposure module containing the lung cells. A microbalance placed within the exposure module estimated the mass of PM that were deposited on the adjacent cells. The pattern of PM deposited on the microbalance resembled the mass pattern collected on the filters (Table 2). The NM229 deposited most particles on the balance followed by NM255 and SS109 respectively. Emissions from both NM255 and NM229 induced cytotoxic effects on the A549 cells of which the emission from NM229 apparently was the most toxic, based on the number of shots. The effect on cell viability was, in addition, estimated as a function of particulate mass deposited on the micro balance. (Table 2). The fumes from NM229 deposited much more PM on the cells but had relatively less effect on the cell viability compared to the masses deposited from the fumes from NM255 (Fig. 4S). This may indicate that factors in the gunshot fumes that do not add to the mass contribute to the toxic effect, such as ultrafine particles or gaseous compounds. Bergström et al. (2015) made a similar experiment, where they tested cytotoxicity of particles from different ammunition types. They collected particles in a liquid and exposed the cells in submerged conditions. They observed that particles sampled from a copper-jacketed steel bullet were most toxic, with an EC_{50} (concentration leading to 50% effect) of 1.9 μg/cm^2. This is a similar concentration level to our experiment. The approach by Bergström et al. (2015) was to expose cells to PM collected in water whereas we exposed the cells directly at ALI conditions, which in principle is a more realistic exposure. However, one major challenge with the ALI approach using an exposure module for both gases and particles,

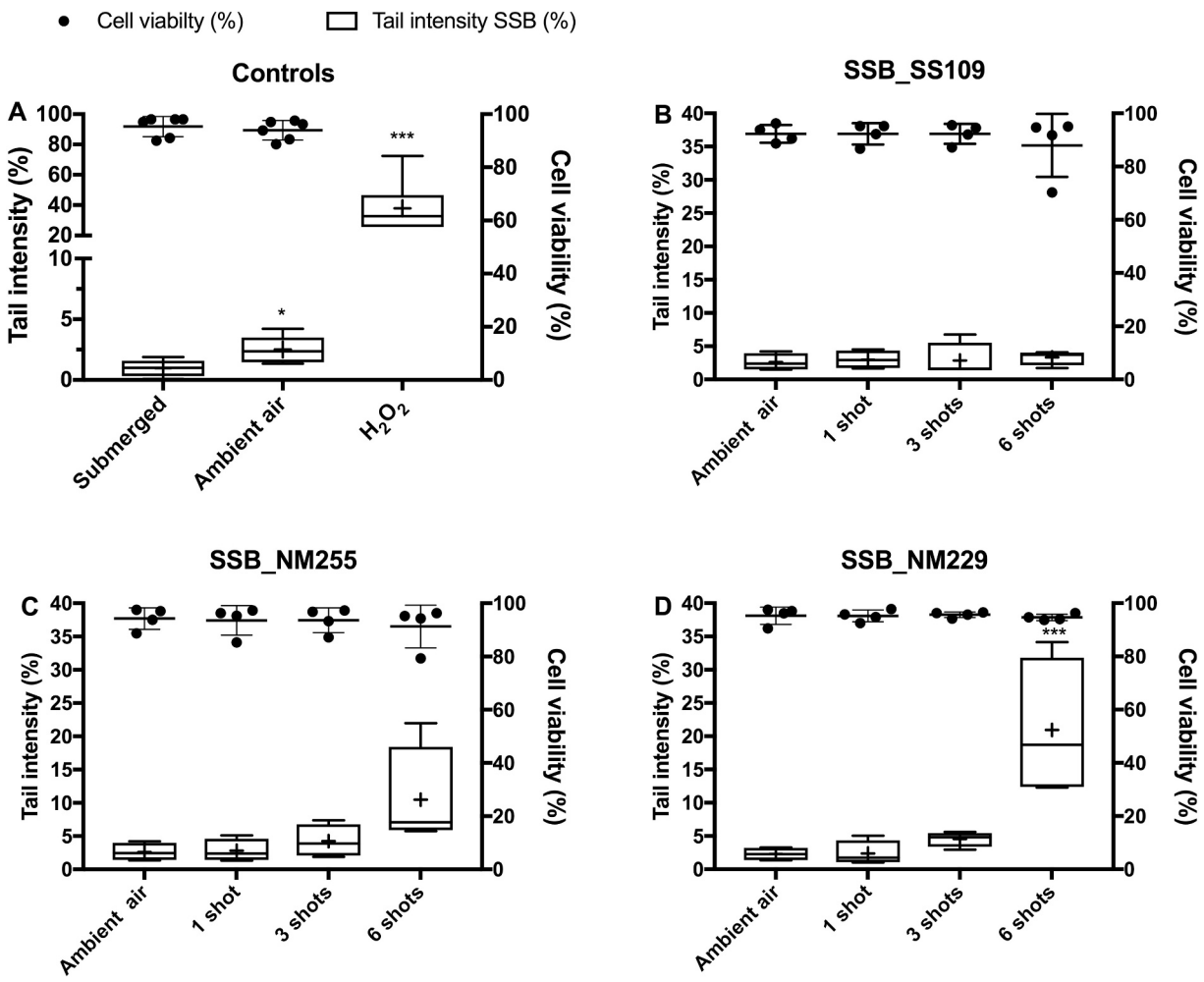

Fig. 7. DNA damage in A549 cells measured by the comet assay shown as single strand breaks (SSB). (A) DNA damage in submerged A549 cells compared to cells exposed at ALI to ambient air at 5 mL/min for 15 min. (B-D) A549 cells exposed to gunshot fumes from three different ammunition types. Results are presented as box plot, with range, median, mean (+) and percentiles from 4 independent experiments. Asterisks indicate significant different effects on cell viability compared to ambient air analysed by one-way ANOVA followed by Dunnet post-test (**p < 0.01). Bullet points show the mean cell viability (± SD) after the exposures measured by trypan blue exclusion assay. (For interpretation of the references to colour in this figure legend, the reader is referred to the web version of this article.)

is to do a reliable characterization of the particles reaching the cells, particularly related to the size distribution of the particles. The particles reaching the cells do probably not resemble the size and distribution characteristics revealed by the impactor and the FMPS measurements. The emitted particles from the gun are led through a tube and then through the exposure module. Some of the smaller sized particles may go through the system, whereas the larger particles may be intercepted and accumulated on turns and walls of the channels. This could be observed visually since considerable amounts of soot and PM accumulated in the tube and in the channels within the exposure module. The cells were also exposed to gases at concentrations resembling what is shown in Fig. 1, which may have contributed to the observed effect. An example is a study by Bakand et al. (2007) who showed that ammonia at 200 ppm was cytotoxic to A549 cells exposed at ALI conditions for 1 h.

High emissions of Cu and Zn are attributed to respiratory distress experienced by soldiers training with the NM229 ammunition type (Voie et al., 2014). Genotoxicity of nanomaterials is regarded as a particularly important aspect of their toxicity (Kohl et al., 2020), as DNA damage can lead to mutation and potentially to the development of cancer. Only the emission from NM229 induced a significant dose-related increase in DNA-damage (one-way ANOVA, $F = 11.1$, $p < 0.001$). Significant effects were, however, only achieved at the highest exposure level (Dunnets post-test, $p < 0.01$), which eventually would lead to reduced cell viability after 24 h of approximately 40%. The effect of the fumes from NM255 showed an increasing trend (one-way ANOVA, $F = 3.1$, $P = 0.067$) and the effect of the fumes from 6 shots reached a significance level of $p = 0.053$ (Dunnets post-test). As for the cytotoxicity experiments, the level of DNA-damage can be attributed to higher mass of PM emitted from this ammunition type. The comet assay was performed immediately after the exposure and detected acute effects on the DNA. For genotoxicity, several endpoints at different DNA organization levels can be assessed, such as DNA base damage, point mutation, large chromosomal damage or aneuploidy (Dusinska et al., 2019). The comet assay measures the disruption of the nucleosomal organization of the DNA leading to relaxation of supercoiled DNA, such as induced by DNA strand breaks (Azqueta and Collins, 2013). This is shown as more DNA in the comet tail. DNA damage is usually efficiently repaired in a cell (*e.g.* Lindahl and Wood, 1999), and damage, such as single strand breaks can be repaired within minutes (*e.g.* Collins and Azqueta, 2012). The DNA damage expressed in this study may therefore represent the instant stress on DNA induced by the gunshot fumes before extensive repair was initiated. The MTT assay showed that some of the damage to the cells ultimately lead to cell death. The observation, however, indicates that exposure to gunshot fumes has the potential to induce permanent DNA damage to lung cells. The effect appeared to be correlated to the particles rather than the formation of gases since the leaded SS109 had

similar emission of gases as the NM229.

In addition to regular COMET measurements of strand breaks, the exposed cells were treated with Fpg. Fpg removes 8-OHgua, leaving apurinic sites that are converted to strand breaks by the associated apurinic endonuclease activity. Formation of 7,8-Dihydro-8-oxo-guanine (8-OHgua) is regarded as an indicator of oxidative stress (Collins et al., 1996). By calculating the net increase in tail intensity following Fpg treatment, there was no significant increase in the strand breaks (Fig. 5S, supplementary) due to formation of 8-OHgua. Oxidative stress has been described as a key mechanism underlying the ability of nanomaterials to cause DNA damage (Magdolenova et al., 2014). The enhanced production of reactive oxygen species can lead to DNA base damage and is considered as one of the most important mechanisms for genotoxicity of nanomaterials (Donaldson et al., 2010). Formation of 8-OHgua is, however, only one of several markers of oxidative stress induced on the DNA and does not rule out that gunshot fumes induce oxidative stress, which may affect the DNA. The lack of effect may also be due to inefficient deposition of the ultrafine particles in the VitroCell system, which are presumed to be the most toxic.

In this study, lung cells were exposed for 15 min at an air rate of 5 mL/min. Taking into account the mass deposited on the micro-balance this implies that the cells were exposed to PM concentrations ranging from 6 to 112 mg/m^3 (Table 2). In the study by Voie et al. (2014) the volunteers were exposed to gunshot fumes from NM229, NM255 and SS109 for one hour. The air concentrations of PM ranged from 10.8 to 17.3 mg/m^3. With a respiratory minute volume of 0.5 L and 12 breaths per min, this implies a maximum total inhalation of 3.9–6.2 mg PM. With an approximate lung surface area of 100 m^2 (Fröhlich et al., 2016) the load is equivalent to 3.9–17.3 ng/cm^2, which is about a factor 1000 less than the cell exposure in this experiment (see Table 2). These numbers are just approximations and assumes that, on a mass basis, all is deposited in the lung, which is not the case. Deposition efficiency of particles in the lung is highly dependent on particle size and shape (Braakhuis et al., 2014; Rissler et al., 2017; Heyder, 2004; Löndahl et al., 2014.

Deposition factors in different regions of the pulmonary system as a function of aerodynamic particle size were calculated according to the MPPD model (Fig. 8A). Based on the calculated deposition factors and the mass-size fraction analysis from the impactor samples, the proportional regional specific lung deposition of metals and soot from the gunshot fumes was estimated (Fig. 8B, Fig. 8S). These estimates indicate that approximately 75% of the Cu and Zn particles, 95% of the Pb particles and approximately 60% of the soot particles that are deposited in the pulmonary system will settle in extrathoracic regions. The study by Sikkeland et al. (2018) showed that some of the respiratory effects from gun smoke fumes can be attributed to effects on the lower respiratory systems, since several of the observed symptoms were systemic. One should, therefore, accommodate further studies on the dynamic and chemical content of the nanosized fraction of the gunshot fumes to reveal the significance of these for the observed health effects.

In conclusion, the emitted fumes from gunshots consist of complicated mixtures of PM and gases, which can be harmful to exposed personnel. Most of the generated PM has, on a number basis, a size distribution of less than 100 nm. The smallest particles will rapidly agglomerate into larger particles, but even several minutes after the firing, there is reason to believe that a substantial portion of the particles have a size distribution that will easily penetrate into the alveolar region of the lungs. The use of the ALI approach is a promising tool to address more realistically potentially toxic effects on the lungs (Upadhyay and Palmberg, 2018). This experiment indicates that the gunshot fumes are cytotoxic to lung cells, and at high concentrations may induce genotoxity. The effects on the lung cells were related to the generated particles from the gunshots, which contain substantial amounts of Cu and Zn. Whether this exposure will induce a permanent effect on the cells or is repaired by the extensive DNA-repair system of the cells remains to be elucidated. In addition to the metals and gases measured in this experiment, gunshot fumes also contain soot and trace amounts of PAHs (Wingfors et al., 2014; Aurell et al., 2019), which may add to the toxicity

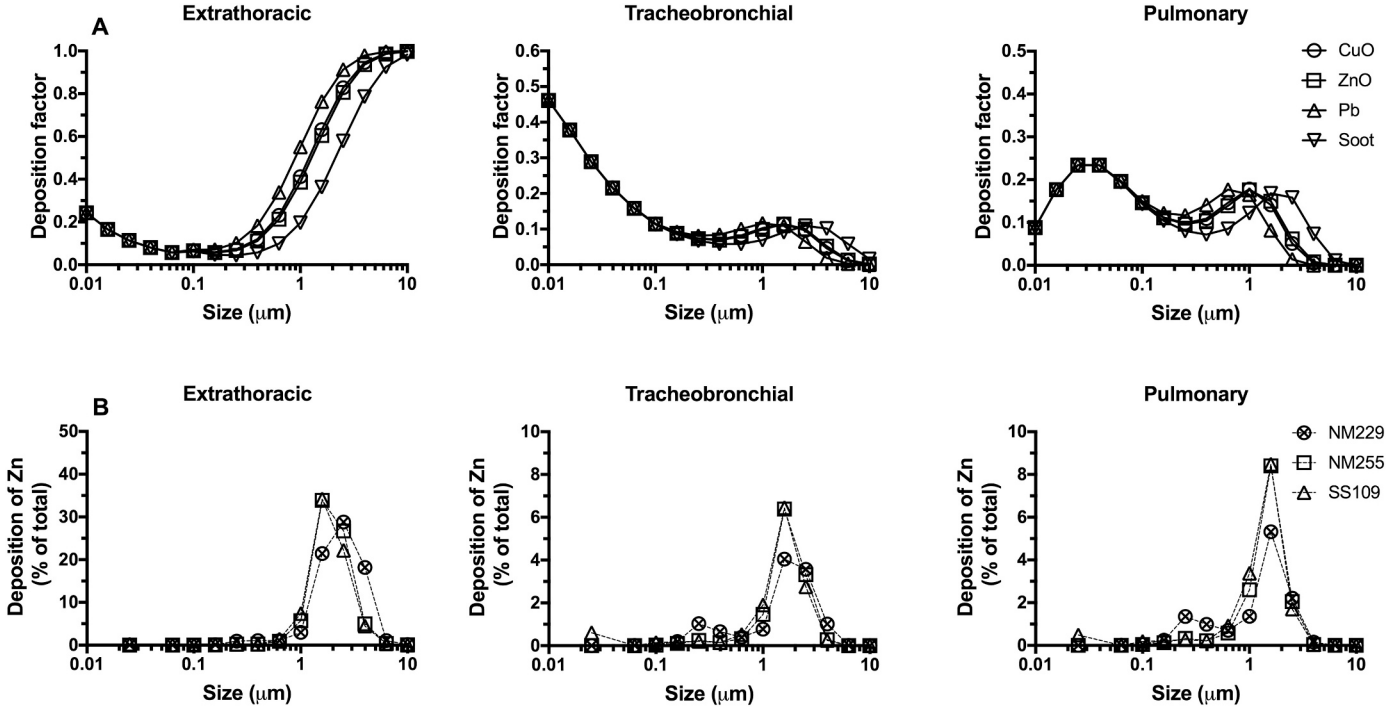

Fig. 8. (A) Regional lung deposition factors of aerosols of CuO (6.31 g/cm^3), ZnO (5.61 g/cm^3), Pb (11.34 g/cm^3) and soot (2 g/cm^3) suspected to be formed in the gunshot fumes calculated according to the MPPD model. The values are means for relaxed nose breathing with tidal volume of 0.5 L and breathing frequency of 12 per min. (B) Estimated cumulative proportion of deposited Zn particles in different lung regions as a function of size based on the mass size fractions of gunshot aerosols and PM sampled on the impactor. The mass fraction of each size range was multiplied with the respective deposition factors calculated in MPPD to reveal which mass size fraction from the fumes with highest relative region-specific deposition.

(Niranjan and Thakur, 2017). There are reasons to believe that repeated exposure to high concentrations of gunshot fumes may induce long lasting effects, which emphasize the importance of extensive ventilation at training areas and to conduct regular lung function testing of repeatedly exposed individuals. The large difference between the concentrations needed to achieve effects *in vitro* compared to real life exposure is, however, a challenge in risk assessment. Development of feasible methodology *in vitro* that can more closely mimic chronic exposure, *e.g.*, through more sensitive endpoints will in the future reduce this gap.

Funding

The study was financed by projects at FFI: Proj. no 1329 FFI: Emission of gases and particles from weapon system. EDA project: TRACE-MI: Toxicological Risk Assessment for Chemical Exposures of Military Interest.

Declaration of Competing Interest

The authors declare no potential conflicts of interest with respect to the research, authorship, and publication of this article.

Acknowledgment

The authors want to acknowledge Dr. Maria Dusinska at NILU for her advices in planning the gene abbreviation assay, and Lasse Sundem-Eriksen at FFI for assistance and guidance in the use of the assault rifle, Arnt Johnsen at FFI for assistance and fruitful discussions. Thanks to Elisabeth Elje at NILU for assisting in the comet experiments, and Jacob Hadler Jacobsen, summer student at FFI, for assisting in the operation of the FMPS and impactor. Thanks also to Paul David Hamer at NILU who kindly edited the manuscript with English corrections.

Appendix A. Supplementary data

Supplementary data to this article can be found online at https://doi.org/10.1016/j.tiv.2021.105095.

Refererences

Anjilvel, S., Asgharian, B., 1995. A multiple-path model of particle deposition in the rat lung. Fundam. Appl. Toxicol. 28, 41–50.
Armbruster, D.A., Tillman, M.D., Hubbs, L.M., 1994. Limit of detection (LOD)/limit of quantification (LOQ): comparison of the empirical and the statistical methods exemplified with GC–MS assays of abused drugs. Clin. Chem. 40, 1233–1238.
Aurell, J., Holder, A.L., Brian, K., Gullett, B.K., Kevin McNesby, K., Weinstein, J.P., 2019. Characterization of M4 carbine rifle emissions with three ammunition types. Environ. Pollut. 254, 112,982.
Azqueta, A., Collins, A.R., 2013. The essential comet assay: a comprehensive guide to measuring DNA damage and repair. Arch. Toxicol. 87, 949–968.
Bakand, S., Winder, C., Hayes, A., 2007. Comparative *in vitro* cytotoxicity assessment of selected gaseous compounds in human alveolar epithelial cells. Toxicol. in Vitro 21, 1341–1347.
Bergström, U., Ekstrand-Hammarström, B., Hägglund, L., Wingfors, H., 2015. Comparing acute toxicity of gunshot particles, from firing conventional and lead-free ammunition, in pulmonary epithelial cell cultures. J. Toxicol. Environ. Health A. 78, 645–661.
Borander, A.K., Voie, Ø.A., Longva, K., Danielsen, T.E., Grahnstedt, S., Sandvik, L., Kongerud, J., Sikkeland, L.I.B., 2017. Military small arms fire in association with acute decrements in lung function. Occup. Environ. Med. 74, 639–644.
Braakhuis, H.M., Park, M.V., Gosens, I., De Jong, W.H., Cassee, F.R., 2014. Physicochemical characteristics of nanomaterials that affect pulmonary inflammation. Part. Fibre Toxicol. 11, 18.
Brede, U., Hagel, R., Redecker, K.H., Weuter, W., 1996. Primer compositions in the course of time: From black powder and SINOXID to SINTOX compositions and SINCO booster. Prop. Explos. Pyrotechn. 21, 113–117.
Collins, A.R., Azqueta, A., 2012. DNA repair as a biomarker in human biomonitoring studies; further applications of the comet assay. Mutat. Res. 736, 122–129.
Collins, A.R., Dusinská, M., Gedik, C.M., Stětina, R., 1996. Oxidative damage to DNA: do we have a reliable biomarker? Environ. Health Perspect. 104 (Suppl. 3), 465–469.
Collins, A.R., Oscoz, A.A., Brunborg, G., Gaivao, I., Giovannelli, L., Kruszewski, M., Smith, C.C., Stetina, R., 2008. The comet assay: topical issues. Mutagenesis 23, 143–151.
Dalen, M.L., Frøyland, E., Saugstad, O.D., Mollnes, T.E., Rootwelt, T., 2009. Post-hypoxic hypothermia is protective in human NT2-N neurons regardless of oxygen concentration during reoxygenation. Brain Res. 1259, 80–89.
Donaldson, K., Poland, C.A., Schins, R.P., 2010. Possible genotoxic mechanisms of nanoparticles: criteria for improved test strategies. Nanotoxicology 4, 414–420.
Dullum, O., Johnsen, A., Sundem-Eriksen, L., 2015. Emission of Gas and Dust from Small Arms. FFI-Report 2015/01728.
Dusinska, M., Mariussen, E., Rundén-Pran, E., Hudecova, A.M., Elje, E., Kazimirova, A., El Yamani, N., Dommershausen, N., Tharmann, J., Fieblinger, D., Herzberg, F., Luch, A., Haase, A., 2019. *In Vitro* approaches for assessing the genotoxicity of nanomaterials. Methods Mol. Biol. 1894, 83–122.
El Yamani, N., Collins, A.R., Rundén-Pran, E., Fjellsbø, L.M., Shaposhnikov, S., Zienolddiny, S., Dusinska, M., 2017. *In vitro* genotoxicity testing of four reference metal nanomaterials, titanium dioxide, zinc oxide, cerium oxide and silver: towards reliable hazard assessment. Mutagenesis 32, 117–126.
Fachehoun, R.C., Lévesque, B., Dumas, P., St-Louis, A., Dubé, M., Ayotte, P., 2015. Lead exposure through consumption of big game meat in Quebec, Canada: risk assessment and perception. Food Addit. Contam. Part A Chem. Anal. Control. Expo. Risk Assess 32, 1501–1511.
Fischbein, A., Rice, C., Sarkozi, L., Kon, S.H., Petrocci, M., Selikoff, I.J., 1979. Exposure to lead in firing ranges. JAMA 241, 1141–1144.
Fröhlich, E., Mercuri, A., Wu, S., Salar-Behzadi, S., 2016. Measurements of deposition, lung surface area and lung fluid for simulation of inhaled compounds. Front. Pharmacol. 7, 181.
Goldberg, R.L., Hicks, A.M., O'Leary, L.M., London, S., 1991. Lead exposure at uncovered outdoor firing ranges. J. Occup. Med. 33, 718–719.
Grabinski, C.M., Methner, M.M., Jackson, J.M., Moore, A.L., Flory, L.E., Tilly, T., Hussain, S.M., Ott, D.K., 2017. Characterization of exposure to byproducts from firing lead-free frangible ammunition in an enclosed, ventilated firing range. J. Occup. Environ. Hyg. 14, 461–472.
Heyder, J., 2004. Deposition of inhaled particles in the human respiratory tract and consequences for regional targeting in respiratory drug delivery. Proc. Am. Thorac. Soc. 1, 315–320.
Kohl, Y., Rundén-Pran, E., Mariussen, E., Hesler, M., El Yamani, N., Longhin, E.M., Dusinska, M., 2020. Genotoxicity of nanomaterials: advanced *in vitro* models and high throughput methods for human hazard assessment– a review. Nanomaterials 10, 1911.
Laidlaw, M.A.S., Filippelli, G., Mielke, H., Gulson, B., Ball, A.S., 2017. Lead exposure at firing ranges-a review. Environ. Health 16, 34.
Lindahl, T., Wood, R.D., 1999. Quality control by DNA repair. Science 286, 1897–1905.
Löndahl, J., Möller, W., Pagels, J.H., Kreyling, W.G., Swietlicki, E., Schmid, O., 2014. Measurement techniques for respiratory tract deposition of airborne nanoparticles: a critical review. J. Aerosol Med. Pulm. Drug Deliv. 27, 229–254.
Magdolenova, Z., Collins, A., Kumar, A., Dhawan, A., Stone, V., Dusinska, M., 2014. Mechanisms of genotoxicity. A review of *in vitro* and *in vivo* studies with engineered nanoparticles. Nanotoxicology 8, 233–278.
Nammo, 2012. Nammo Bulletin 2012.
Nammo, 2014. Nammo Ammunition Handbook, , 2nd Ed2014.
Niranjan, R., Thakur, A.K., 2017. The toxicological mechanisms of environmental soot (Black Carbon) and carbon black: focus on oxidative stress and inflammatory pathways. Front. Immunol. 8, 763.
Palmer, W.G., Andrews, A.W., Mellini, D., Terra, J.A., Hoffmann, F.J., Hoke, S.H., 1994. Mutagenicity of particulate emissions from the M16 rifle: variation with particle size. J. Toxicol. Environ. Health 42, 423–433.
Rissler, J., Gudmundsson, A., Nicklasson, H., Swietlicki, E., Wollmer, P., Löndahl, J., 2017. Deposition efficiency of inhaled particles (15–5000 nm) related to breathing pattern and lung function: an experimental study in healthy children and adults. Part. Fibre Toxicol. 14, 10.
Sikkeland, L.I.B., Borander, A.K., Voie, Ø.A., Aass, H.C.D., Øvstebø, R., Aukrust, P., Longva, K., Alexis, N.E., Kongerud, J., Ueland, T., 2018. Systemic and airway inflammation after exposure to fumes from military small arms. Am. J. Respir. Crit. Care Med. 197, 1349–1353.
Strømseng, A.E., Voie, Ø.A., Johnsen, A., Bergsrud, S.M., Parmer, M.P., Røen, B.T., Ljønes, M., Johannessen, C., Longva, K.S., 2009. Helseplager i forbindelse med bruk av. HK416 – vurdering av. årsak og helserisiko. [Norwegian] FFI-report 2009/00820.
Upadhyay, S., Palmberg, L., 2018. Air-liquid interface: relevant *in vitro* models for investigating air pollutant-induced pulmonary toxicity. Toxicol. Sci. 164, 21–30.
Valway, S.E., Martyny, J.W., Miller, J.R., Cook, M., Mangione, E.J., 1989. Lead absorption in indoor firing range users. Am. J. Public Health 79, 1029–1032.
Voie, Ø., Borander, A.K., Sikkeland, L.I., Grahnstedt, S., Johnsen, A., Danielsen, T.E., Longva, K., Kongerud, J., 2014. Health effects after firing small arms comparing leaded and unleaded ammunition. Inhal. Toxicol. 26, 873–879.
Wingfors, H., Svensson, K., Hägglund, L., Hedenstierna, S., Magnusson, R., 2014. Emission factors for gases and particle-bound substances produced by firing lead-free small-calibre ammunition. J. Occup. Environ. Hyg. 11, 282–291.